Molecular Cancer Therapeutics

Epithelial-to-mesenchymal transition mediates docetaxel resistance and high risk of relapse in prostate cancer

Mercedes Marín-Aguilera, Jordi Codony-Servat, Òscar Reig, et al.

Mol Cancer Ther Published OnlineFirst March 21, 2014.

Epithelial-to-mesenchymal transition mediates docetaxel resistance and high risk of relapse in prostate cancer

Mercedes Marín-Aguilera[1*], Jordi Codony-Servat[1*], Òscar Reig[1], Juan José Lozano[3], Pedro Luis Fernández[4,2], María Verónica Pereira[1], Natalia Jiménez[1], Michael Donovan[5], Pere Puig[5], Lourdes Mengual[6], Raquel Bermudo[2,7], Albert Font[8], Enrique Gallardo[9], María José Ribal[6], Antonio Alcaraz[6,2], Pere Gascón[1,2], Begoña Mellado[1,2].

*Equally contributed to this work

Authors' affiliation:
[1]Laboratory of Translational Oncology and Medical Oncology Department, Hospital Clínic, Barcelona, Spain.
[2]Institut d'Investigacions Biomèdiques August Pi i Sunyer (IDIBAPS), Barcelona, Spain.
[3]Bioinformatics Platform Department, Centro de Investigación Biomédica en Red - Enfermedades Hepáticas y Digestivas (CIBEREHD), Hospital Clínic, Barcelona, Spain.
[4]Department of Pathology, Hospital Clínic, Universitat de Barcelona, Spain.
[5]Althia, Barcelona, Spain.
[6]Laboratory and Department of Urology, Hospital Clínic. Institut d'Investigacions Biomèdiques August Pi i Sunyer (IDIBAPS), Universitat de Barcelona, Spain
[7] Tumor Bank, Hospital Clínic – IDIBAPS Biobank, Barcelona, Spain
[8]Medical Oncology Department, Hospital Germans Trias i Pujol, Catalan Institute of Oncology, Badalona, Spain.
[9]Medical Oncology Department, Hospital Parc Taulí, Sabadell, Spain.

Running title: EMT role in docetaxel resistance

Keywords: Docetaxel, EMT, Prostate cancer, Resistance, *ZEB1*

Abbreviation list:

AD Androgen deprivation

AR	Androgen receptor
Cq	Quantification cycle
CRPC	Castration-resistant prostate cancer
D	Docetaxel
EMT	Epithelial-to-mesenchymal transition
FC	Fold change
FFPE	Formalin-fixed paraffin-embedded
H&E	Hematoxylin and eosin
IF	Immunofluorescence
IHC	Immunohistochemistry
PC	Prostate cancer
pCR	pathological complete response
PSA	prostate-specific antigen
PA	Pre-amplification

Financial support

This work was supported by Cellex Foundation, by the Instituto de Salud Carlos III - Subdirección General de Evaluación y Fomento de la Investigación (grants number PI07/0388 and PI12/01226; IP recipient B. Mellado), and by the Ministerio de Economía y competitividad (grant number SAF2012-40017-C02-02; IP recipient P.L. Fernández). This study was also cofinanced by Fondo Europeo de Desarrollo Regional. Unión Europea. *Una manera de hacer Europa*. M. Marín-Aguilera received a grant from Cellex Foundation. This work was developed at the Centro Esther Koplowitz, Barcelona, Spain.

Corresponding Author:

Begoña Mellado

Medical Oncology Department

Hospital Clínic de Barcelona

Villarroel 170, Barcelona, 08036, Spain.

Phone: 34-93-227-5400, ext. 2262;

Fax: 34-93-454-6520;

E-mail: bmellado@clinic.ub.es

Disclosure of Potential Conflicts of Interest: The authors have declared no conflicts of interest.

Word count: Abstract: 250; Manuscript: 4742

Total number of figures and tables: 6 (plus 1 supplementary table and 2 supplementary figures)

ABSTRACT

Molecular characterization of radical prostatectomy specimens after systemic therapy may identify a gene expression profile for resistance to therapy. This study assessed tumor cells from patients with prostate cancer (PC) participating in a phase-II neoadjuvant docetaxel (D) and androgen deprivation (AD) trial to identify mediators of resistance. Transcriptional level of 93 genes from a D-resistant PC cell lines microarray study was analyzed by Taqman low-density arrays in tumors from patients with high-risk localized PC (36 surgically treated, 28 with neoadjuvant D+AD). Gene expression was compared between groups and correlated with clinical outcome. VIM, AR and P65 were validated by immunohistochemistry. CD44 and ZEB1 expression was tested by immunofluorescence in cells and tumor samples. Parental and D-resistant CRPC cell lines were tested for epithelial-to-mesenchymal transition (EMT) markers before and after D-exposure. Reversion of EMT phenotype was investigated as a D-resistance reversion strategy. Expression of 63 (67.7%) genes differed between groups (P<0.05), including genes related to androgen receptor, NFKB transcription factor, and EMT. Increased EMT markers expression correlated with radiological relapse. D-resistant cells had increased EMT and stem-like cell markers expression. *ZEB1* siRNA transfection reverted D-resistance and reduced *CD44* expression in DU-145R and PC-3R. Before D-exposure, a selected $CD44^+$ subpopulation of PC-3 cells exhibited EMT phenotype and intrinsic D-resistance; $ZEB1/CD44^+$ subpopulations were found in tumor cell lines and primary tumors; this correlated with aggressive clinical behavior.

This study identifies genes potentially related to chemotherapy resistance and supports evidence of the EMT role in docetaxel resistance and adverse clinical behavior in early PC.

Introduction

Prostate cancer (PC) is the most common malignancy in the Western world and the second most common cause of cancer-related mortality in men (1). Although most metastatic PC patients respond to androgen deprivation (AD) therapy, virtually all of them eventually develop castration-resistant prostate cancer (CRPC). In 2004, the combination of docetaxel (D) and prednisone was established as the new standard of care for CRPC patients (2). More recently, two hormonal agents, abiraterone and enzalutamide, and a new taxane, cabazitaxel, have been approved for the treatment of CRPC (3-5). However, current therapies are not curative and research is needed to identify predictors of benefit and mechanisms of resistance for each agent.

To date, several factors have been associated with D-resistance, including expression of isoforms of ß-tubulin (6), activation of drug efflux pumps (7), *PTEN* loss (8), and expression and/or activation of survival factors (i.e. PI3-K/Akt and mTOR) (9, 10). Previous work by our group and others has correlated the activation of Nuclear Factor Kappa B (NFKB)/interleukin-6 pathways with D-resistance in CRPC models and in patients (11-13). Other studies support a role of Jun/AP-1, SNAIL1, and Notch2/Hedgehog signaling pathways in the development of resistance to D or paclitaxel (14, 15). Moreover, it has been shown that the inhibition of Androgen receptor (AR) nuclear translocation and AR activity may be an important mechanism of taxane action in PC (9).

In previous work, we identified 243 genes with differential expression in CRPC D-sensitive *vs* D-resistant cell lines (16). In the present study, 73 genes from that study together with 20 genes from the literature were tested in tumor specimens of high-risk, localized-PC patients included in a clinical trial of

neoadjuvant hormone-chemotherapy (17), and compared with nontreated specimens with similar clinical characteristics. This approach was based on the notion that residual tumor cells in prostatectomy specimens after neoadjuvant systemic therapy are likely enriched for resistant tumor cells and their molecular characterization may provide important information on mechanisms of resistance (18). Our key findings were then tested in two models of D-resistant PC cell lines.

PATIENTS AND METHODS

Patients and samples

The study included 28 high-risk, localized-PC patients from a previously published, multicenter, phase II trial of neoadjuvant D plus AD followed by radical prostatectomy (17) and 36 control patients with high-risk PC treated with radical prostatectomy without neoadjuvant treatment. Of the 57 participants in the clinical trial (17), 29 were not included in this study: 23 patients did not consent to participation in the molecular sub-study and insufficient material for molecular analysis was available for 6 patients, 3 of whom had a pathological complete response (pCR) and 3 had microscopic residual tumor (near pCR) in the prostate specimen.

Inclusion criteria were histologically confirmed adenocarcinoma of the prostate with any of the following three risk criteria: [1] clinical stage T3; [2] clinical stage T1c or T2 with serum prostate-specific antigen (PSA) >20 ng ml−1 and/or Gleason score sum of 8, 9 or 10; or [3] a Gleason sum of 7 with a predominant form of 4 (i.e. Gleason score 4+3). Clinical characteristics are shown in Table 1.

Treatment consisted of three cycles every 28 days of D 36□mg□/m2 on days 1, 8, and 15 concomitant with complete androgen blockade, followed by radical prostatectomy. Patients were followed from the time of study inclusion until death or last visit. Median follow-up time was 82 months (range, 10-135). PSA relapse was defined as two consecutive values of 0.2 ng/mL or greater (19). Radiological progression was defined as the progression in soft tissue lesions measured by computed tomography or magnetic resonance imaging, or by progression to bone (20).

The study was approved by each participating hospital's Institutional Ethics committee and written informed consent was obtained from all participants. Formalin-fixed paraffin-embedded (FFPE) specimens were collected after radical prostatectomy. A representative tumor area was selected for each block and, according to its size, between 2 and 12 sections were cut, 10 µm thick, and used for RNA isolation. Hematoxylin and Eosin (H&E) stained sections from tumors and adjacent tissues were prepared to confirm the histological diagnosis.

RNA extraction

Total RNA was isolated from tumor specimens using the RecoverAll Total Nucleic Acid Isolation Kit (Life Technologies) according to the manufacturer's protocol. Total RNA was quantified with a spectrophotometer (NanoDrop Technologies).

Gene selection

In total, 93 target genes that could potentially be related to D-resistance and two endogenous control genes (*ACTINB* and *GUSB*) were selected for further analysis in tumors. A set of 73 target genes was selected for their relative expression in docetaxel-resistant cells (DU-145R and PC-3R) *vs* parental cells (DU-145 and PC-3) (16) using DAVID (21) and IPA software (http://www.ingenuity.com). Twenty genes highlighted in the literature as potential targets of docetaxel resistance were also selected.

Reverse transcription and pre-amplification

A High-Capacity cDNA Reverse Transcription kit (Life Technologies) was used to reverse-transcribe 1 µg of total RNA in a 50 µl reaction volume. cDNA pre-amplification (PA) was performed by multiplex PCR with the 93 selected genes (Supplementary Table S1) and the stem-like cell markers *CD24* and *CD44*, following the manufacturer's instructions for the TaqMan PreAmp Master Mix Kit (Life Technologies), except that final volume of the reaction was 25 µl.

Gene expression analysis in FFPE samples

Pre-amplified cDNA was used for gene expression analysis using 384-Well Microfluidic Cards (Life Technologies). Pre-amplified samples were diluted 1:20 in TE 1X buffer before use. Each card was configured into four identical 96-gene sets (95 selected genes plus an endogenous control gene, *RNA18S*, by default). The reaction was carried out following manufacturer's instructions on an ABI 7900HT instrument (Life Technologies). Array cards were analyzed with RQ Manager Software for manual data analysis.

Gene expression of *CD24* and *CD44* markers was studied by amplifying with TaqMan Gene Expression Master Mix in a StepOnePlus Real-Time PCR system (Life Technologies), according to the manufacturer's recommendations. Relative gene expression values were calculated based on the quantification cycle (Cq) values obtained with SDS 2.4 software (Life Technologies). Expression values were relative to the *GUSB* endogenous gene. Samples from patients who did not receive neoadjuvant treatment were used for calibration.

Cell culture conditions

The CRPC cell lines DU-145 and PC-3 were purchased from the American Type Culture Collection in October 2009. The D-resistant cell lines DU-145R and PC-3R were developed and maintained as previously described (12). No further authentication of the cell lines was done by the authors.

Cell proliferation assays

Cell viability in response to D was assessed by 3-(4,5-dimethylthiazol-2yl-2,5-diphenyltetrazolium bromide (MTT) assay with the Cell Titer 96 Aqueous Proliferation assay kit (Promega, Madison, WI) and by trypan blue exclusion method using a Neubauer hemocytometer chamber.

Western Blot Analysis

Whole-cell extracts were prepared and Western blot performed as described previously (22). Antibodies used were Anti-Poly-(ADP-Ribose)-Polymerase (PARP). Ab was purchased from Roche (Ref. 11835238001 - Basel, Switzerland); β-Catenin (6B3) (CTNNB1) Ab (Ref.9582), CD44 (156-3C11)

Mouse mAb (Ref.3570), E-cadherin (CDH1) Ab (Ref.4065), Snail (C15D3) Rabbit mAb (Ref.3879), TCF8/ZEB1 (D80D3) Rabbit mAb (Ref.3396), and Vimentin (R28) (VIM) Ab (Ref.3932) were purchased from Cell Signaling Technologies (Beverly, MA). Monoclonal Anti- α-Tubulin clone B-5-1-2 (Ref.T5168) was purchased from Sigma-Aldrich (St. Louis, MO).

Real-time qRT-PCR in cell lines

Total RNA was isolated from cell lines using the RNeasy Micro kit (Qiagen), and quantified with a spectrophotometer (Nanodrop Technologies). cDNA was generated from 1 μg of total RNA using the High Capacity cDNA Archive Kit (Life Technologies), following manufacturer's instructions. Real-time qRT-PCR was carried out in a StepOnePlus Real-Time PCR system (Life Technologies) according to the manufacturer's recommendations. Data were acquired using SDS Software 1.4. Amplification reactions were performed in duplicate. Expression values were relative to the *ACTB* endogenous gene. Target genes were amplified using commercial primers and probes (Life Technologies) (Supplementary Table S1).

Immunohistochemistry (IHC)

Tissue sections were deparaffinized in xylene and rehydrated in graded alcohols. For AR and VIM staining, the sections were placed in a 97ºC solution of 0.01 mol/L EDTA (pH 9.0) for antigen retrieval. Primary mouse mononuclear antibody for AR (DAKO, Agilent Technologies, US) was applied for 20 minutes at room temperature at dilution 1:150. FLEX Monoclonal Mouse Anti-VIM, Clon V9 (DAKO) was used for VIM staining. Detection was accomplished with the

DAKO Envision System followed by diaminobenzidine enhancement. For P65, the sections were placed in a 97ºC solution of 0.01 mol/L sodium citrate (pH 6.0) for antigen retrieval. Then, samples were incubated with a rabbit polyclonal antibody (Santa Cruz biotechnology, Inc, US) at dilution 1:400. Detection was performed with Bond Polymer Refine Detection (DAKO, Agilent Technologies, US) for the automated Bond system.

AR and P65 were evaluated throughout the semiquantitative method histological score (HSCORE), which measures both the intensity and proportion of staining. The HSCORE for each sample was calculated by multiplying the percentage of stained tumor cells by the intensity (0: non-stained; 1: weak; 2: moderate; 3: strong). VIM was evaluated in the same way but scoring the percentage of staining on a scale of 0 to 4 (0: 0; 1: <1%; 2: 1-9%; 3: 10-50%; 4: >50%). Nuclear and cytoplasmatic stains were scored separately for AR and P65 proteins. The assessment of all samples was done by a senior pathologist (P.L.-F) who was blinded to all clinical information.

Immunofluorescence staining in cell lines and tumor samples

Cell pellets were collected in a 1% agarose solution, fixed in 4% PBS-buffered formaldehyde, and then formalin-fixed and paraffin-embedded. Sections of 5 μm were analyzed with a multiplex immunofluorescent assay. They were stained with Hematoxylin and Eosin (H&E) for histopathologic assessment and stained using immunofluorescence (IF) with Alexa fluorochrome-labeled antibodies. Briefly, both control and resistant PC cell lines were evaluated with a series of simplex and duplex IF assays to quantify the level of selected antibody-antigen complexes from specific regions of interest (ROI).

The FFPE prostate tissue sections also were assessed by IF using a single multiplex assay with 2 differentially labeled antibodies (ZEB1 and CD44). For all specimens the H&E images were used to guide and register IF image capture with a maximum of 4 ROIs per cell pellet and 6 per tissue section. Alexa fluorochrome dyes were Vimentin (Ref. MO725, Dako), CD44 (Ref.: 156-3C11, Cell Signaling Technology), ZEB1 (Ref.: sc-25388, Santa Cruz). The ROI were acquired from the cells and tumor tissue sections, blinded to outcome, with a CRI Nuance imaging system, and then analyzed with fluorescent image analysis software to derive quantitative features from cellular/tissue compartments. Quantitative assessment was performed using a pixel-area function, normalized to the ROI under investigation.

Small interfering RNA transfection

Dharmacon SMART pool control and *ZEB1* siRNA were used with lipofectamine according to the manufacturer's protocol (Thermo Scientific) to inhibit ZEB1 in DU-145/R cells. Commercial Silencer Select siRNA of ZEB1 (s229971; Life Technologies) was transfected to PC-3/R cell lines. Cells were incubated with the siRNA complex for 24 hours, treated with D, then harvested to study protein expression changes of ZEB1 and CDH1 by Western blot. Apoptosis was studied at 24 and 48 hours by PARP analysis (Western blot), and cell viability was measured by MTT at 72 hours as described before.

Fluorescence-activated cell sorting (FACS)

For flow cytometry, cells were dissociated with Accutase (Invitrogen) and washed twice in a serum-free medium. Cells were stained live in the staining

solution containing BSA and FITC-conjugated monoclonal anti-CD44 (15 min at 4 ºC). A minimum of 500,000 viable cells per sample were analyzed on a cytometer. For FACS, 2-5 x 10^7 cells were similarly stained for CD44 and used to sort out $CD44^+$ and $CD44^-$ cells. For the positive population, only the top 10% mostly brightly stained cells were selected. The $CD44^+$ cells selected were cultured as an individual clone in 96-well plates and expanded.

Statistical Analysis

TLDAs gene expression data was evaluated by Wilcoxon rank-sum test and receiver operating characteristic analysis. Time to PSA progression and radiological progression were calculated from the time of prostate cancer diagnosis until PSA or radiological progression, respectively. The log-rank test was used in univariate survival analyses. Multivariate analysis of gene expression was evaluated by Cox proportional hazards regression including stage, Gleason, PSA and neoadjuvant treatment as clinical covariates; backward stepwise likelihood was used for selection. Real-time qRT-PCR experimental data was expressed as mean $\pm$ SEM and was analyzed by Student *t* test. All the statistical tests were conducted at the two-sided 0.05 level of significance.

RESULTS

Differential gene expression between treated and nontreated tumors

Among the 93 genes analyzed (Supplementary Table S1), we observed differential expression ($P < 0.05$) in 63 (67.7%) genes (Table 2); 53 genes were overexpressed and 10 under-expressed in tumor specimens from patients

treated with neoadjuvant D plus AD. Genes of the NFKB pathway (such as *NFKB1*, *REL*, *RELA*), AR and epithelial-to-mesenchymal transition (EMT)-related genes (such as *ZEB1*, *VIM*, *CDH2, TGFBR3*) were overexpressed in treated tumors. Among the down-regulated genes in treated tumors, were the metastasis suppressor gene *NDRG1* (23) and the adhesion molecule *EPCAM*, a regulator of the alternative splicing of *CD44* (*ESRP1*) (24) and *ST14* (a negative regulator of the EMT mediator *ZEB1*) (25)(Table 2, Fig. 1A).

Gene expression and clinical outcome

We tested the possible prognostic impact of the 93 genes studied by TLDAs (Supplementary Table S1). Individually, the expression of several genes was related to time-to-PSA and/or clinical relapse (Table 2). Time to radiological progression and PSA progression curves are shown in Figure 1B, 1C and Supplementary Figures S1 and S2. Of note, the overexpression of *AR,* and the EMT-related genes *TGFBR3*, *ZEB1*, and *VIM* was correlated with a shorter time of radiological progression (Fig. 1B).

We then performed a multivariate analysis including the genes with individual prognostic value, clinical prognostic factors (PSA, Gleason, and clinical stage), and neo-adjuvant treatment. Results are shown in table 2A and 2B. In the multivariate analysis, the reduced expression of *CLDN7* was an adverse independent prognostic factor for clinical relapse. Loss of *CLDN7* has been correlated with adverse prognostic variables in PC and with EMT (26). Of note, the low expression of *CDH1* was an independent prognostic factor for time to PSA relapse.

We also analyzed the prognostic impact of the stem-like cell markers *CD24* and *CD44,* which were underexpressed and overexpressed, respectively, in treated tumors (FC CD24: 0.59, *P*=0.07; FC CD44: 1.63, *P*<0.000) (Supplementary table 1 and supplementary figure 1 and 2). Of note, low expression of CD24 was correlated with shorter time of biochemical progression (Fig. 1C).

Immunohistochemistry in treated *vs* nontreated tumors

We explored the expression of VIM and both cytoplasmatic and nuclear P65 and AR in tumor samples from neoadjuvant-treated and non-treated patients. Staining of cytoplasmatic P65 was significatively higher in the treated vs non-treated patients (IHC score 181.9 vs 148.3, respectively) (Fig. 1D,F). Moreover, nuclear P65 was significantly related to worse clinical relapse (Fig. 1E). Vimentin expression was nonsignificantly higher in treated tumors (IHC score 2 vs 1, respectively) (Fig. 1D). No differences were found in the expression of nuclear AR; however, cytoplasmatic AR expression was significantly higher in the treated tumors (IHC score 102.5 vs 14.5) and correlated with radiological progression survival (Fig. 1D,E,F).

D-resistant prostate cancer cells express EMT and stem-like cell markers

Based on the results described above, we studied the link between EMT and D-resistance in four PC cell lines models (parental DU-145 and PC-3R cells, and their docetaxel-resistant partners DU-145R and PC-3R, respectively). As shown in Figure 2A and 2B, the D-resistant cells phenotype was consistent with EMT, i.e., decreased expression of epithelial markers (CDH1 and CTNNB1) and increased expression of mesenchymal markers (VIM and ZEB1) at the protein

level. Consistent results were found at mRNA level, except for CTNNB1 (data not shown).

Recent studies have shown that cells with EMT phenotype share characteristics of stem-like cancer cells (14, 27). For that reason we tested the expression of stem-like cell markers and showed that D-resistant cells, both DU-145R and PC-3R, exhibit transcriptional features of cancer-stem cells, such as increased expression of *CD44* and the loss of *CD24* (Fig. 2C).

Moreover, in cell lines we detected by IF analysis a subset of cells co-expressing *CD44* and ZEB1. Scattered cells with these features were detectable in the parental cell lines; however, this population was highly enriched in the resistant cells (Fig. 2D). By FACS, we then isolated from the parental PC-3 cells a subpopulation of cells with high expression of CD44. We selected a derived-$CD44^{+}$/PC-3 clone that showed an increased expression of *VIM* and *ZEB1* and decreased *CDH1* expression (Fig. 2E). This clone from the parental cells was significantly more resistant to D than the parental cell line, PC-3 (Fig. 2F).

Dose-response experiments in both parental and resistant cells showed that D exposure significantly increased the expression of *VIM* in PC-3 and PC-3R cells, of *ZEB1* in PC-3 cells, and of *SNAI1* in DU-145, PC-3 and PC-3R cells. *TWIST1* expression increased in all cell lines after D treatment. In contrast, no significant differences were observed in the expression of *SNAI2* and *CDH1* with D exposure (Fig. 3A). Regarding stem-like cell markers, inconsistent results were obtained for *CD24* expression after D exposure because CD24 expression increased in PC-3 cells but decrease in DU-145 cells. In contrast, CD44 significantly increased in PC-3 cells with D treatment (Fig. 3B).

EMT mediates docetaxel resistance in prostate cancer cells

To test whether inhibition of EMT could revert D resistance, we down-modulated the expression of ZEB1, a key inducer of EMT. siRNA ZEB1 transfected DU-145R and PC-3R cells had an increased expression of CDH1 (Fig. 4A) and CD44 (Fig. 4B), confirming the link between EMT and stem-like cell phenotype. Moreover, si-RNA ZEB1 transfected cells showed significantly increased sensitivity to D compared to control cells ($P < 0.05$) (Fig. 4B and 4C). The magnitude of the reversion of chemoresistance was more pronounced in DU-145R and PC-3R cells than in the parental cells. D-induced apoptosis was more pronounced in the ZEB1-siRNA transfected cells (Fig. 4B).

ZEB1/CD44 expression in tumor samples

Based on preclinical findings, we decided to investigate whether $CD44^+/ZEB1^+$ cells were present in primary PC specimens. Twenty-two FFPE tumors from high-risk PC patients treated with D and androgen suppression and 15 control patients with sufficient remaining material were available for IF studies. All samples were positive for CD44 staining but only 7 of 15 controls (46.7%) and 7 of 22 treated patients (31.8%) had a ZEB1 signal. Overall, there were no differences between the control and treated groups in the expression of ZEB1 (0.0059 *vs* 0.013 mean intensity, respectively) or CD44 (1.27 *vs* 1.01 mean intensity, respectively). Tumor cells that co-expressed ZEB1 and $CD44^+$ were observed in 3 (13.6%) of the 22 patients in the neoadjuvant group. However, none of the control patients presented with co-expression of both markers (Fig. 4D). Notably, ZEB1/CD44 co-expression was associated with aggressive clinical behavior: at the time of outcome analysis, all patients had relapsed, 2

had developed liver metastasis, and 1 had died due to disease progression (Fig. 4E).

DISCUSSION

In this study we confirm that some of the molecular alterations associated with D-resistance in a previously described *in vitro* model of CRPC cell lines are present in residual cells of prostatectomy specimens treated with neoadjuvant D plus AD. Our findings may be especially relevant in clinical practice because most patients receive AD prior and concomitantly to the administration of D. The observed deregulated pathways may translate common mechanisms of resistance to both therapies.

Different neoadjuvant studies have been designed to identify pathways involved in resistance to AD or chemotherapy in PC. In one study of neoadjuvant AD, the authors observed that many androgen-responsive genes, including AR and PSA, were not suppressed; this suggests that suboptimal suppression of tumoral androgen activity may lead to adaptive cellular changes to allow PC cells survival in a low-androgen environment (28). Another group analyzed prostate tumors removed by radical prostatectomy after 3 months of AD. Gene expression analysis revealed that PSA and other androgen-responsive genes were overexpressed in tumors from patients who relapsed (29). Our data are in concordance with these reports. We observed that the expression of AR and several AR-regulated genes (i.e, *ZEB1*, *IL6*, *TGFBR3*, *KLF9*) increased in treated tumors, even though serum PSA levels decreased under therapy in most cases, as we previously reported (17). Moreover, high levels of AR correlated with high risk of clinical-relapse. These data suggest that persistence

of AR signalling may be related to treatment resistance and/or to eventual disease progression.

We observed no differences in nuclear staining between treated and non-treated samples. However, cytoplasmatic expression was significantly higher in residual tumor cells after AD and D exposure. Prior reports have shown that taxanes inhibit AR nuclear translocation and that patients treated with taxanes may have lower nuclear expression than treatment-naïve patients (30). This was not observed in our study, likely because our patients were treated with combined therapy. Prior studies have shown that androgen deprivation induced full-length androgen receptor protein levels in CRPC cells, but decreased its nuclear localization (31).

Other studies have used a similar approach in patients treated with neoadjuvant chemotherapy alone (32, 33). One group performed microarray analysis of tumor specimens from 31 patients treated with D plus mitoxantrone (33). The comparison of pre- and post-treatment samples showed increased expression of cytokines regulated by the NFKB pathway. These data are in concordance with our results showing an increased expression in treated tumors of NFKB subunits and NFKB regulated cytokines, such as IL6, adding support to a body of evidence on the involvement of this pathway in resistance to chemotherapy in PC (11). On the other hand, NFKB activation may induce EMT in PC (34). Although our study did not investigate the potential causal relationship between NFKB activation and EMT, this last phenomenon was found to be highly relevant in resistance to therapy. Moreover, increased nuclear NFKB (P65 staining) correlated with a shorter time to clinical relapse, confirming the prognostic value of this pathway activation in PC (22).

In the present study we analyze the transcriptional profile of residual tumor cells after combined neoadjuvant AD and D treatment. Since macrodissected tumor tissues were used for gene expression studies, our results may translate expression patterns from both tumor and surrounding non-tumor cells. However, a prior study using the macrodissection strategy reported only minor interference of non-tumor cells with the overall gene expression profile (35). Moreover, we considered stroma and benign cells contamination to be homogeneous in both the treated and non-treated patient groups. Among the 93 genes analyzed, we observed differential expression between treated and nontreated tumors in 63 (67.7 %) genes. Of note, the over expression of the EMT genes correlated with a shorter time to clinical relapse.

In the EMT process, cells lose epithelial characteristics and gain mesenchymal properties to increase motility and invasion, allowing tumor cells to acquire the capacity to infiltrate surrounding tissues and to metastasize in distant sites. EMT is typically characterized by the loss of epithelial (i.e. *CDH1*) and the gain of mesenchymal (i.e. *VIM*, *CDH2*) markers expression (36). Several reports suggest that AR activation, as well as androgen deprivation therapy, may induce changes characteristic of EMT that may be involved in PC progression (37-39). The expression of the transcription factor *ZEB1* may be induced by dihydrotestosterone and is mediated by two androgen-response elements (40). Recently, Sun et al. showed that androgen deprivation causes EMT in animal models and in tumor samples of patients treated with hormone therapy (41). Moreover, the presence of AR-truncated isoforms, which are increased in the castration-resistant progression, regulate the expression of EMT (42).

On the other hand, there are molecular similarities between cancer stem-like cells and EMT-phenotypic cells. Moreover, cells with an EMT phenotype induced by different factors are rich sources for stem-like cancer cells (14, 27). We observed in the DU-145 *in vitro* model that D-resistant cells expressed high levels of the stem-cell marker CD44 and decreased levels of CD24. Moreover, D treatment increased CD44 expression in tumor cells. Likewise, RT-PCR results in tumor samples showed an increased expression of *CD44* and a decreased expression of *CD24* in tumors treated with neoadjuvant AD plus D. Our results are in accordance with those of Puhr et al, who detected an increased CD24low-CD44high cell population in D-resistant PC models (43). Similarly, Li et al detected CD24low-CD44high breast cancer cells that were resistant to neoadjuvant chemotherapy (44). In a preclinical study, CD44 and CD147 enhanced metastatic capacity and chemoresistance of PC cells, potentially mediated by activation of the PI3K and MAPK pathways (45).

In the present work we identified a population of PC cells exhibiting an EMT phenotype that are primarily resistant to D. The presence of an intrinsic resistant cell population was supported by the isolation of D-resistant clonal cells in the parental cell line PC-3, before D exposure, with a high expression of CD44 and EMT markers and the loss of *CDH1*. $ZEB1^{+}/CD44^{+}$ cells were identified at a very low frequency in the two parental cell lines, DU-145 and PC3, before D exposure but their frequency massively increased in D-resistant cells. Similarly, a small percentage of $ZEB1^{+}/CD44^{+}$ cells were also observed in primary high-risk localized PC tumors. $ZEB1^{+}/CD44^{+}$ cells were present only in tumors that had previously received neoadjuvant AD plus D (13.6%). Both in vitro and tumor sample findings support the presence of primary resistant cells

harboring EMT/stem cell-like characteristics and suggest that the exposure to D may eliminate sensitive cells resulting, however, in the selective out-growth of this resistant cell population.

In our model, D also induced EMT changes in the parental and resistant cell lines. Based on our findings, both mechanisms, the existence of a primary resistant cell with an EMT phenotype and the induction of EMT changes induced by D, are possible. In recent work on D-resistant PC-3 and DU-145 derived cell lines, the authors reported that D-resistant cells underwent an EMT transition associated with a reduction of microRNA (miR)-200c and miR-205, which regulate the epithelial phenotype. Their study also showed reduced *CDH1* expression in tumors after neoadjuvant chemotherapy (43). Another study showed that paclitaxel-DU-145 resistant cells have greater *ZEB1*, *VIM,* and *SNAI1* expression (46).

We tested whether EMT played a causal role in D chemoresistance by interfering with the expression of the transcription factor ZEB1, a key mediator of EMT, in PC cell lines. We observed that ZEB1 genetic down-modulation restored CDH1 but suppressed CD44 expression, which was consistent with a reversion of EMT and stem-like cell features. We also observed that ZEB1 inhibition caused PC cell mortality independently of D. This effect was previously described and is consistent with the known role of ZEB1 in cell proliferation related, which is related to the expression of cell cycle inhibitory cyclin-dependent kinase inhibitors (47). Furthermore, ZEB1 inhibition restored sensitivity to D, supporting a mechanistic role of EMT and stem-like cell phenotype in resistance to therapy. In a previous study of an adenocarcinoma lung cancer model, inhibition of ZEB1 significantly enhanced the

chemosensitivity of D-resistant cells *in vitro*, and *in vivo* the ectopic expression of ZEB1 increased chemoresistance (48).

Several reports have provided evidence that EMT is critical for invasion and migration and is involved in tumor recurrence, which is believed to be tightly linked to cancer stem cells. CD44 and VIM expression in primary tumors has been correlated with adverse prognosis (34, 49). Notably, the few patients in our series with $ZEB1^{+}/CD44^{+}$ tumor cells in primary tumors showed extremely aggressive clinical behavior.

In summary, we observed a differential expression of NFKB, AR, EMT and stem-like cell markers between treated and not-treated tumors. Moreover, they were related to a higher risk of PSA and/or clinical relapse. Since the neoadjuvant population may be of higher risk than the surgical patients, we cannot exclude the possibility that the expression of these markers is more related to the characteristics of the disease than to the therapy. However, none of the clinical factors (PSA, Gleason, clinical stage, or the presence of prior neoadjuvant therapy) correlated with clinical outcome in the univariate or multivariate analysis in our series.

Overall, our findings support a role of EMT in resistance to PC therapy and progression. Our clinical data were generated in the neoadjuvant setting and cannot be extrapolated to CRPC patients. However, both *in vitro* and clinical results support the investigation of the role of EMT in resistance to chemotherapy in CRPC. Moreover, novel strategies to revert or prevent EMT are warranted to improve the outcome of CRPC or to increase the probabilities of cure for high-risk PC patients.

ACKNOWLEDGMENTS

The authors thank Instituto de Salud Carlos III and Cellex Foundation for funding the project. The authors also would like to thank Mónica Marín and Laura Gelabert for their excellent technical assistance and Elaine Lilly, Ph.D., for review of the English text.

REFERENCES

1. Siegel R, Naishadham D, Jemal A. Cancer statistics for Hispanics/Latinos, 2012. CA Cancer J Clin 2012;62:283-98.

2. Tannock IF, de WR, Berry WR, Horti J, Pluzanska A, Chi KN, et al. Docetaxel plus prednisone or mitoxantrone plus prednisone for advanced prostate cancer. N Engl J Med 2004;351:1502-12.

3. Ryan CJ, Smith MR, de Bono JS, Molina A, Logothetis CJ, de SP, et al. Abiraterone in metastatic prostate cancer without previous chemotherapy. N Engl J Med 2013;368:138-48.

4. Scher HI, Fizazi K, Saad F, Taplin ME, Sternberg CN, Miller K, et al. Increased survival with enzalutamide in prostate cancer after chemotherapy. N Engl J Med 2012;367:1187-97.

5. de Bono JS, Oudard S, Ozguroglu M, Hansen S, Machiels JP, Kocak I, et al. Prednisone plus cabazitaxel or mitoxantrone for metastatic castration-resistant prostate cancer progressing after docetaxel treatment: a randomised open-label trial. Lancet 2010;376:1147-54.

6. Ploussard G, Terry S, Maille P, Allory Y, Sirab N, Kheuang L, et al. Class III beta-tubulin expression predicts prostate tumor aggressiveness and patient response to docetaxel-based chemotherapy. Cancer Res 2010;70:9253-64.

7. Fojo T, Menefee M. Mechanisms of multidrug resistance: the potential role of microtubule-stabilizing agents. Ann Oncol 2007;18 Suppl 5:v3-v8.

8. Antonarakis ES, Keizman D, Zhang Z, Gurel B, Lotan TL, Hicks JL, et al. An immunohistochemical signature comprising PTEN, MYC, and Ki67 predicts progression in prostate cancer patients receiving adjuvant docetaxel after prostatectomy. Cancer 2012;118:6063-71.

9. Darshan MS, Loftus MS, Thadani-Mulero M, Levy BP, Escuin D, Zhou XK, et al. Taxane-induced blockade to nuclear accumulation of the androgen receptor predicts clinical responses in metastatic prostate cancer. Cancer Res 2011;71:6019-29.

10. Guertin DA, Sabatini DM. Defining the role of mTOR in cancer. Cancer Cell 2007;12:9-22.

11. Domingo-Domenech J, Oliva C, Rovira A, Codony-Servat J, Bosch M, Filella X, et al. Interleukin 6, a nuclear factor-kappaB target, predicts resistance to docetaxel in hormone-independent prostate cancer and nuclear factor-kappaB inhibition by PS-1145 enhances docetaxel antitumor activity. Clin Cancer Res 2006;12:5578-86.

12. Codony-Servat J, Marin-Aguilera M, Visa L, Garcia-Albeniz X, Pineda E, Fernandez PL, et al. Nuclear factor-kappa B and interleukin-6 related docetaxel resistance in castration-resistant prostate cancer. Prostate 2013;73:512-21.

13. Shen MM, bate-Shen C. Molecular genetics of prostate cancer: new prospects for old challenges. Genes Dev 2010;24:1967-2000.

14. Kurrey NK, Jalgaonkar SP, Joglekar AV, Ghanate AD, Chaskar PD, Doiphode RY, et al. Snail and slug mediate radioresistance and chemoresistance by antagonizing p53-mediated apoptosis and acquiring a stem-like phenotype in ovarian cancer cells. Stem Cells 2009;27:2059-68.

15. Domingo-Domenech J, Vidal SJ, Rodriguez-Bravo V, Castillo-Martin M, Quinn SA, Rodriguez-Barrueco R, et al. Suppression of acquired docetaxel resistance in prostate cancer through depletion of notch- and hedgehog-dependent tumor-initiating cells. Cancer Cell 2012;22:373-88.

16. Marin-Aguilera M, Codony-Servat J, Kalko SG, Fernandez PL, Bermudo R, Buxo E, et al. Identification of docetaxel resistance genes in castration-resistant prostate cancer. Mol Cancer Ther 2012;11:329-39.

17. Mellado B, Font A, Alcaraz A, Aparicio LA, Veiga FJ, Areal J, et al. Phase II trial of short-term neoadjuvant docetaxel and complete androgen blockade in high-risk prostate cancer. Br J Cancer 2009;101:1248-52.

18. Seruga B, Ocana A, Tannock IF. Drug resistance in metastatic castration-resistant prostate cancer. Nat Rev Clin Oncol 2011;8:12-23.

19. Boccon-Gibod L, Djavan WB, Hammerer P, Hoeltl W, Kattan MW, Prayer-Galetti T, et al. Management of prostate-specific antigen relapse in prostate cancer: a European Consensus. Int J Clin Pract 2004;58:382-90.

20. Scher HI, Halabi S, Tannock I, Morris M, Sternberg CN, Carducci MA, et al. Design and end points of clinical trials for patients with progressive prostate cancer and castrate levels of testosterone: recommendations of the Prostate Cancer Clinical Trials Working Group. J Clin Oncol 2008;26:1148-59.

21. Huang dW, Sherman BT, Lempicki RA. Systematic and integrative analysis of large gene lists using DAVID bioinformatics resources. Nat Protoc 2009;4:44-57.

22. Domingo-Domenech J, Mellado B, Ferrer B, Truan D, Codony-Servat J, Sauleda S, et al. Activation of nuclear factor-kappaB in human prostate carcinogenesis and association to biochemical relapse. Br J Cancer 2005;93:1285-94.

23. Sun J, Zhang D, Bae DH, Sahni S, Jansson P, Zheng Y, et al. Metastasis suppressor, NDRG1, mediates its activity through signaling pathways and molecular motors. Carcinogenesis 2013;34:1943-54.

24. Yae T, Tsuchihashi K, Ishimoto T, Motohara T, Yoshikawa M, Yoshida GJ, et al. Alternative splicing of CD44 mRNA by ESRP1 enhances lung colonization of metastatic cancer cell. Nat Commun 2012;3:883.

25. Gemmill RM, Roche J, Potiron VA, Nasarre P, Mitas M, Coldren CD, et al. ZEB1-responsive genes in non-small cell lung cancer. Cancer Lett 2011;300:66-78.

26. Sheehan GM, Kallakury BV, Sheehan CE, Fisher HA, Kaufman RP, Jr., Ross JS. Loss of claudins-1 and -7 and expression of claudins-3 and -4 correlate with prognostic variables in prostatic adenocarcinomas. Hum Pathol 2007;38:564-9.

27. Mani SA, Guo W, Liao MJ, Eaton EN, Ayyanan A, Zhou AY, et al. The epithelial-mesenchymal transition generates cells with properties of stem cells. Cell 2008;133:704-15.

28. Mostaghel EA, Page ST, Lin DW, Fazli L, Coleman IM, True LD, et al. Intraprostatic androgens and androgen-regulated gene expression persist after testosterone suppression: therapeutic implications for castration-resistant prostate cancer. Cancer Res 2007;67:5033-41.

29. Ryan CJ, Smith A, Lal P, Satagopan J, Reuter V, Scardino P, et al. Persistent prostate-specific antigen expression after neoadjuvant androgen depletion: an early predictor of relapse or incomplete androgen suppression. Urology 2006;68:834-9.

30. Zhu ML, Horbinski CM, Garzotto M, Qian DZ, Beer TM, Kyprianou N. Tubulin-targeting chemotherapy impairs androgen receptor activity in prostate cancer. Cancer Res 2010;70:7992-8002.

31. Gowda PS, Deng JD, Mishra S, Bandyopadhyay A, Liang S, Lin S, et al. Inhibition of hedgehog and androgen receptor signaling pathways produced synergistic suppression of castration-resistant prostate cancer progression. Mol Cancer Res 2013;11:1448-61.

32. Febbo PG, Richie JP, George DJ, Loda M, Manola J, Shankar S, et al. Neoadjuvant docetaxel before radical prostatectomy in patients with high-risk localized prostate cancer. Clin Cancer Res 2005;11:5233-40.

33. Huang CY, Beer TM, Higano CS, True LD, Vessella R, Lange PH, et al. Molecular alterations in prostate carcinomas that associate with in vivo exposure to chemotherapy: identification of a cytoprotective mechanism involving growth differentiation factor 15. Clin Cancer Res 2007;13:5825-33.

34. Zhang Q, Helfand BT, Jang TL, Zhu LJ, Chen L, Yang XJ, et al. Nuclear factor-kappaB-mediated transforming growth factor-beta-induced expression of vimentin is an independent predictor of biochemical recurrence after radical prostatectomy. Clin Cancer Res 2009;15:3557-67.

35. de Bruin EC, van de PS, Lips EH, van ER, van der Zee MM, Lombaerts M, et al. Macrodissection versus microdissection of rectal carcinoma: minor influence of stroma cells to tumor cell gene expression profiles. BMC Genomics 2005;6:142.

36. Nauseef JT, Henry MD. Epithelial-to-mesenchymal transition in prostate cancer: paradigm or puzzle? Nat Rev Urol 2011;8:428-39.

37. Jennbacken K, Tesan T, Wang W, Gustavsson H, Damber JE, Welen K. N-cadherin increases after androgen deprivation and is associated with metastasis in prostate cancer. Endocr Relat Cancer 2010;17:469-79.

38. Zhu ML, Kyprianou N. Role of androgens and the androgen receptor in epithelial-mesenchymal transition and invasion of prostate cancer cells. FASEB J 2010;24:769-77.

39. Matuszak EA, Kyprianou N. Androgen regulation of epithelial-mesenchymal transition in prostate tumorigenesis. Expert Rev Endocrinol Metab 2011;6:469-82.

40. Anose BM, Sanders MM. Androgen Receptor Regulates Transcription of the ZEB1 Transcription Factor. Int J Endocrinol 2011;2011:903918.

41. Sun Y, Wang BE, Leong KG, Yue P, Li L, Jhunjhunwala S, et al. Androgen deprivation causes epithelial-mesenchymal transition in the prostate: implications for androgen-deprivation therapy. Cancer Res 2012;72:527-36.

42. Cottard F, Asmane I, Erdmann E, Bergerat JP, Kurtz JE, Ceraline J. Constitutively active androgen receptor variants upregulate expression of mesenchymal markers in prostate cancer cells. PLoS One 2013;8:e63466.

43. Puhr M, Hoefer J, Schafer G, Erb HH, Oh SJ, Klocker H, et al. Epithelial-to-mesenchymal transition leads to docetaxel resistance in prostate cancer and is mediated by reduced expression of miR-200c and miR-205. Am J Pathol 2012;181:2188-201.

44. Li M, Knight DA, Smyth MJ, Stewart TJ. Sensitivity of a novel model of mammary cancer stem cell-like cells to TNF-related death pathways. Cancer Immunol Immunother 2012;61:1255-68.

45. Hao J, Madigan MC, Khatri A, Power CA, Hung TT, Beretov J, et al. In vitro and in vivo prostate cancer metastasis and chemoresistance can be modulated by expression of either CD44 or CD147. PLoS One 2012;7:e40716.

46. Kim JJ, Yin B, Christudass CS, Terada N, Rajagopalan K, Fabry B, et al. Acquisition of paclitaxel resistance is associated with a more aggressive and invasive phenotype in prostate cancer. J Cell Biochem 2013;114:1286-93.

47. Liu Y, Sanchez-Tillo E, Lu X, Huang L, Clem B, Telang S, et al. The ZEB1 Transcription Factor Acts in a Negative Feedback Loop with miR200 Downstream of Ras and Rb1 to Regulate Bmi1 Expression. J Biol Chem 2013.

48. Ren J, Chen Y, Song H, Chen L, Wang R. Inhibition of ZEB1 reverses EMT and chemoresistance in docetaxel-resistant human lung adenocarcinoma cell line. J Cell Biochem 2013;114:1395-403.

49. Patrawala L, Calhoun T, Schneider-Broussard R, Li H, Bhatia B, Tang S, et al. Highly purified CD44+ prostate cancer cells from xenograft human tumors are enriched in tumorigenic and metastatic progenitor cells. Oncogene 2006;25:1696-708.

TABLES

Table 1: Clinical characteristics of patients. N/A: Not available; [1]Missing information; [2]In some cases Gleason score could not be assessed because of tissue changes related to neoadjuvant treatment.

		All	Neoadjuvant treatment	Control
Total number		64	28	36
Median age (years)		64 (range, 46 - 74)	64 (range, 48 - 70)	64.5 (range, 46 - 74)
Clinical Stage	T1	19 (29.7%)	4 (14.3%)	15 (41.7%)
	T2	33 (51.6%)	14 (50%)	18 (50%)
	T3	12 (18.8%)	10 (35.7%)	3 (8.3%)
Pathological Stage	T0	1 (1.6%)	1 (3.6%)	0
	T1	1 (1.6%)	1 (3.6%)	0
	T2	26 (40.6%)	13 (46.4%)	13 (36.1%)
	T3	36 (56.3%)	13 (46.4%)	23 (63.9%)
Gleason score (Biopsy)	≤ 6	10 (15.6%)	2 (7.1%)	8 (22.2%)
	7 (3+4)	22 (34.4%)	7 (25%)	15 (41.7%)
	7 (4+3)	16 (25%)	8 (28.6%)	8 (22.2%)
	7(N/A[1])	-	-	1 (2.8%)
	8	11 (17.2%)	8 (28.6%)	3 (8.3%)
	9	4 (6.3%)	3 (10.7%)	1 (2.8%)
Gleason score (Prostatectomy)	N/A[2]	18 (28.3%)	18 (64.3%)	0
	≤ 6	7 (15.2%)	7 (25%)	0
	7 (3+4)	13 (20.3%)	1 (3.6%)	12 (33.3%)
	7 (4+3)	17 (26.6%)	-	17 (47.2%)
	8	2 (4.3%)	0	2 (5.6%)
	9	7 (15.2%)	2 (7.1%)	5 (13.9%)
Median PSA (ng/ml)		8.7 (range, 2.01 - 41)	12.2 (range, 4.7 - 41)	8.2 (range, 2.01 - 19.2)
PSA (ng/ml)	< 20	56 (87.5)	20 (71.4%)	36 (100%)
	> 20	8 (12.5%)	8 (28.6%)	0 (0%)
Postoperative radiotherapy	No	35 (58.3%)	13 (54.2%)	22 (61.1%)
	Yes	24 (40%)	10 (41.7%)	14 (38.9%)
	N/A[1]	1 (1.7%)	1 (4.2%)	0 (0%)
Biochemical relapse	No	30 (46.9%)	11 (39.3%)	19 (52.8%)
	Yes	34 (53.1%)	17 (60.7%)	17 (47.2%)
Median biochemical relapse free survival (months)		31.7 (range, 4 - 81)	29.3 (range 4 - 59)	34.1 (range, 8 - 81)
Clinical relapse	No	58 (90.6%)	22 (78.6%)	36 (100%)
	Yes	6 (9.4%)	6 (21.4%)	0 (0%)
Median clinical relapse free survival (months)		51.2 (range, 31 - 84)	51.2 (range, 31 - 84)	-
Follow-up (months)		82 (range, 10 - 135)	91 (range, 81 - 96)	69 (range, 10 - 135)

Table 2: Multivariate analysis of gene expression and patient outcomes. bPFS: biochemical progression-free survival; rPFS: radiological progression-free survival; False discovery rate for differentially expressed genes was < 0.074 in all cases; FC: Fold change; [a]Significant Cox regression analysis; HR: Hazard ratio; 95%CI: 95% confidence interval. $P < 0.05$.

	Gene	FC	Progression	Multivariate[a] HR; CI95%	Gene	FC	Progression	Multivariate[a] HR; CI95%	Gene	FC	Progression	Multivariate[a] HR; CI95%
Differentially expressed genes	*TGFBR3*	4.48	rPFS		*ABCB1*	2.46	-		*NFKB1*	1.76	bPFS	
	SERPINB5	4.43	-		*CDH2*	2.45	-		*AR*	1.73	rPFS	
	CST6	4.19	-		*LTB*	2.40	-		*PTPRM*	1.71	-	
	CLDN11	3.69	rPFS. bPFS	3.056 (1.169-7.988) rPFS	*TIMP2*	2.38	rPFS		*REL*	1.68	bPFS	
	GPR87	3.65	bPFS		*ID2*	2.38	-		*KLF9*	1.50	rPFS	
	AREG	3.42	-		*EFEMP1*	2.35	rPFS		*BRCA1*	1.47	-	
	SCD5	3.32	rPFS		*FRMD3*	2.32	-		*SMAD4*	1.36	bPFS	0.163 (0.058-0.457)
	TMEM45A	3.30	rPFS		*HTRA1*	2.31	-		*FRMD4A*	1.31	-	
	MAP7D3	3.23	-		*LAMC2*	2.22	bPFS	0.131 (0.027-0.634)	*GSPT2*	1.29	-	
	VIM	3.23	rPFS		*SLC1A3*	2.17	rPFS. bPFS	2.555 (1.088-5.999) rPFS	*FN1*	1.20	-	
	BCL2A1	3.09	-		*ZEB1*	2.16	rPFS		*GOSR2*	1.16	-	
	PLSCR4	3.01	rPFS		*IFI16*	2.15	-		*NDRG1*	-1.27	-	
	SCARA3	3.01	-		*EGFR*	2.11	-		*BTBD11*	-1.41	bPFS	0.321 (0.143-0.720)
	ITGB2	2.92	-		*SAMD9*	2.09	-		*CCNB1*	-1.41	-	
	SAMD12	2.80	rPFS. bPFS		*FBN1*	2.03	-		*ESRP1*	-1.46	-	
	S100A4	2.80	rPFS		*FAS*	1.91	-		*FBP1*	-1.53	-	
	G0S2	2.79	-		*TACSTD2*	1.83	-		*EPCAM*	-1.73	-	
	SLCO4A1	2.75	rPFS		*RELA*	1.81	rPFS		*AIM1*	-1.98	-	
	SNAI1	2.71	-		*TXNIP*	1.77	rPFS		*FLJ27352*	-2.09	rPFS. bPFS	0.257 (0.113-0.584) rPFS
	IL6	2.64	rPFS	0.112 (0.015-0.856) rPFS	*KLHL24*	1.77	rPFS		*ST14*	-2.19	rPFS	
	LOC401093	2.49	-		*EML1*	1.76	rPFS		*C1orf116*	-6.08	rPFS	
Non-differentially expressed genes	*CBLB*	ns	bPFS	0.315 (0.143-0.695)	*CSCR7*	ns	bPFS	0.241 (0.077-0.755)	*RAB40B*	ns	bPFS	0.314 (0.134-0.739)
	CCPG1	ns	bPFS	0.263 (0.118-0.585)	*EPS8L1*	ns	bPFS		*SCEL*	ns	rPFS	
	CDH1	ns	bPFS	0.446 (0.217-0.917)	*IGF1R*	ns	bPFS		*SERPINA1*	ns	rPFS	0.032 (0.002-0.632)
	CDK19	ns	rPFS		*LOC401093*	ns	rPFS		*TP53INPL*	ns	rPFS	
	CLDN7	ns	rPFS	0.054 (0.004-0.699)	*MALAT1*	ns	rPFS. bPFS	0.361 (0.141-0.921) rPFS				

FIGURE LEGENDS

Figure 1: Gene expression profile and related outcome of patients treated with neoadjuvancy *vs* nontreated patients. **A.** Heatmap of differentially expressed genes in tumor samples from neoadjuvant-treated patients, compared to those without treatment ($P < 0.05$). Rows represent genes and columns represent samples. Red pixels: upregulated genes; Green pixels: downregulated genes; **B.** Radiological progression-free survival analysis of patients according to gene expression of *AR* and the EMT-related markers *TGFBR3*, *ZEB1* and *VIM*. High and low expression was established according to ROC curve analysis. Log-rank test was used to assess the statistical difference between the two groups ($P < 0.05$); **C.** Kaplan-Meier curve representing biochemical progression-free survival analysis of patients according to gene expression of the stem-like cell marker CD24. High and low expression was established according to ROC curve analysis. Log-rank test was used to assess the statistical difference between the two groups ($P < 0.05$); **D.** Immunohistochemistry (IHC) of VIM and nuclear and cytoplasmatic P65 and AR. Box plot represents IHC scores for each protein. *$P < 0.05$. **E.** Kaplan-Meier graphs representing radiological progression-free survival analysis of patients according to cytoplasmatic AR and P65 nuclear staining by IHC. Log-rank test was used to assess the statistical difference between the two groups ($P < 0.05$); **F.** Images show representative immunohistochemical staining for nuclear P65 and cytoplasmatic AR protein in prostate cancer tumors. Magnifications illustrate high and low staining of cells.

Figure 2: EMT and stem cell markers in parental and D-resistant cell lines. **A.** Western blot in DU-145, DU-145R, PC-3 and PC-3R cell lines of epithelial

markers (CDH1, CTNNB1) and mesenchymal markers (VIM, ZEB1). Tubulin was used as a load control; **B.** Gene expression of EMT markers by qRT-PCR in DU-145, DU-145R, PC-3, and PC-3R cell lines. Data shown is the mean ± SEM of cell lines from triplicate experiments (*$P < 0.05$); **C.** Gene expression of stem-cell markers by qRT-PCR in DU-145, DU-145R, PC-3, and PC-3R cell lines. Data shown is the mean ± SEM of cell lines from triplicate experiments (*$P < 0.05$); **D.** Confocal immunofluorescence of CD44 (red) and ZEB1 (green) in DU-145, DU-145R, PC-3, and PC-3R lines. Colocalization of ZEB1 and CD44 results are in yellow. Nuclei are stained with DAPI (blue); **E.** Western blot in parental PC-3 and a subpopulation of parental PC-3 cells (clone) sorted by CD44 marker. Tubulin was used as a load control; **F.** Viability assay of PC-3 and PC-3 clone under docetaxel treatment performed by Tripan Blue method (*$P < 0.05$).

Figure 3: Effect of docetaxel exposure on EMT and stem-like gene expression markers in prostate cancer cell lines. **A.** EMT markers gene expression in a docetaxel dose-response manner; **B.** Stem-like cell markers gene expression in a docetaxel dose-response manner; Geometrical symbols represent significant differences in the corresponding cell line; data from DU-145 0nM was considered the reference for all the other measures (ie FC=1).

Figure 4: Inhibition of ZEB1 in parental and docetaxel-resistant cell lines. ZEB1-CD44 staining in prostate tumor specimens. **A.** Western blot of CDH1 and ZEB1 in the four cell lines (DU-145, DU-145R, PC-3 and PC-3R) when ZEB1 was inhibited by siRNA. **B.** Western blot of CD44 and PARP in the four

cell lines (DU-145, DU-145R, PC-3 and PC-3R transfected cells) treated with docetaxel; the band of CD44 in PC-3 and PC-3R corresponds to the variant CD44v6; **C.** MTT of ZEB1-siRNA transfected cells. Data represents mean ± SEM of triplicate experiments. *P < 0.05; **D.** CD44 and ZEB1 immunofluorescence image of a prostate tumor biopsy from a patient treated with neoadjuvant docetaxel and androgen deprivation; **E.** Kaplan-Meier according to immunofluorescence intensities of CD44–ZEB1 colocalization and clinical/biochemical relapse of patients treated with neoadjuvant docetaxel and controls without neoadjuvant treatment.

C: non-trasnfected cells; Lipo: control lipofectamine; si: siRNA-ZEB1.

Author Manuscript Published OnlineFirst on March 21, 2014; DOI: 10.1158/1535-7163.MCT-13-0775
Author manuscripts have been peer reviewed and accepted for publication but have not yet been edited.

Figure 1

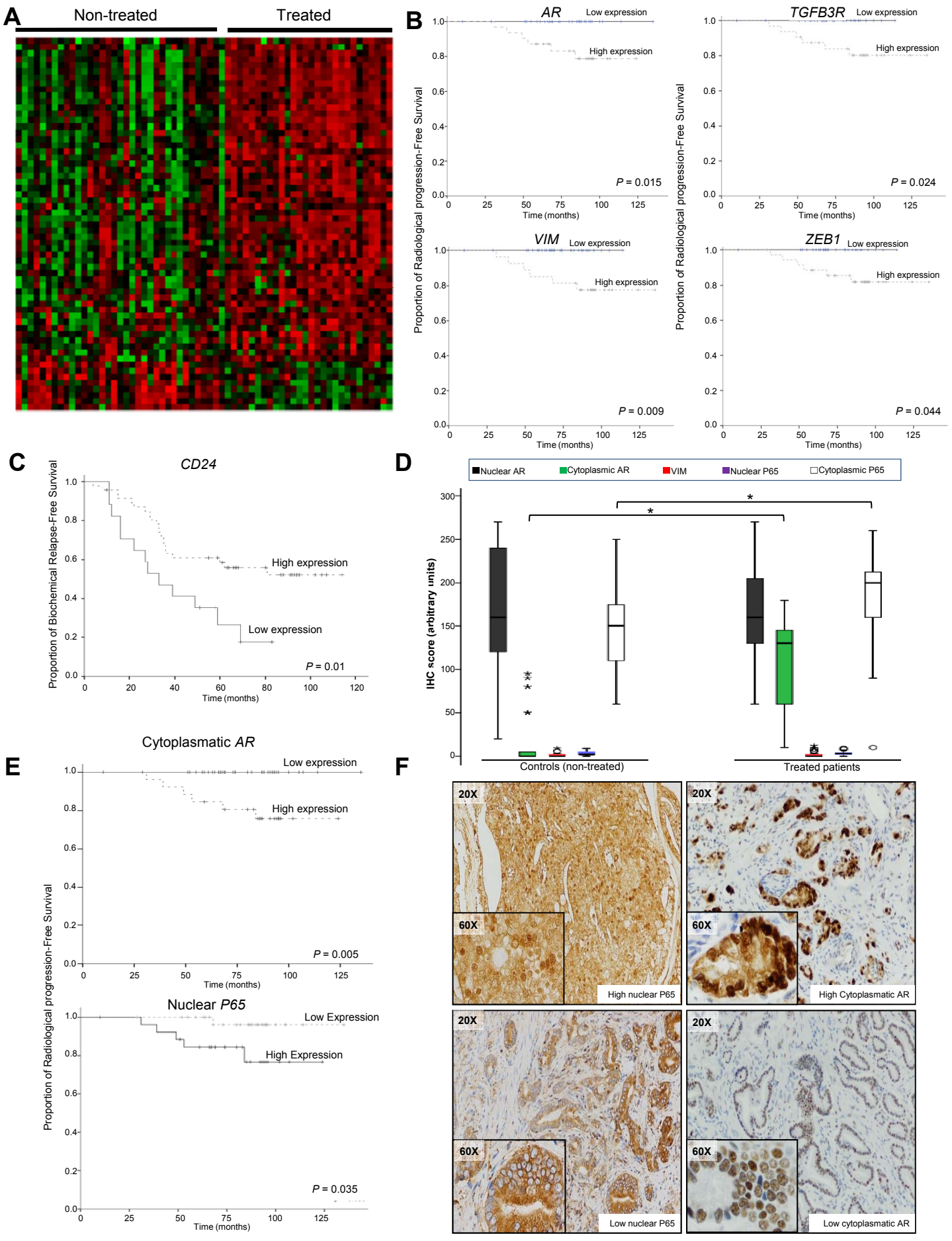

Author Manuscript Published OnlineFirst on March 21, 2014; DOI: 10.1158/1535-7163.MCT-13-0775
Author manuscripts have been peer reviewed and accepted for publication but have not yet been edited.

Figure 2

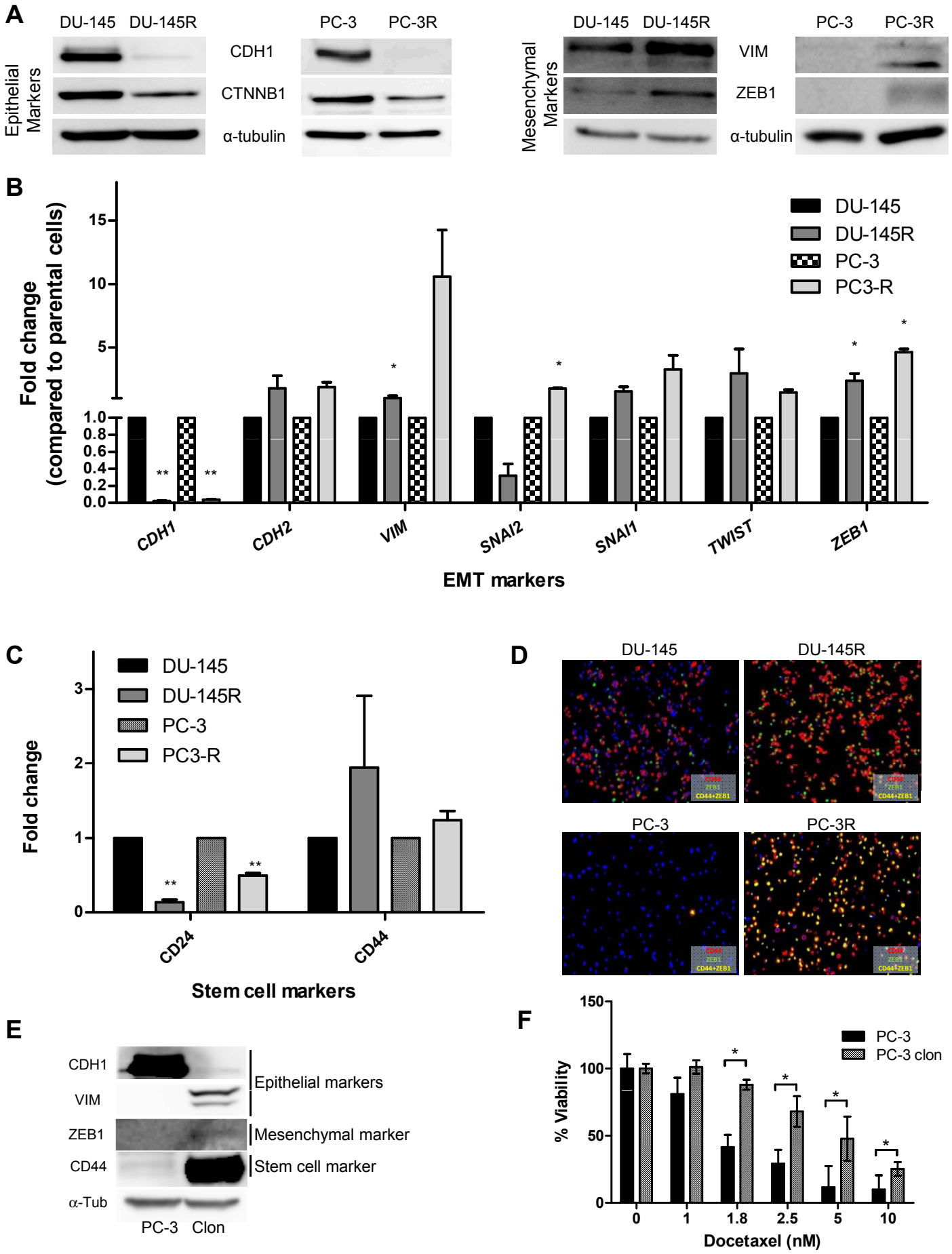

Author Manuscript Published OnlineFirst on March 21, 2014; DOI: 10.1158/1535-7163.MCT-13-0775
Author manuscripts have been peer reviewed and accepted for publication but have not yet been edited.

Figure 3

A

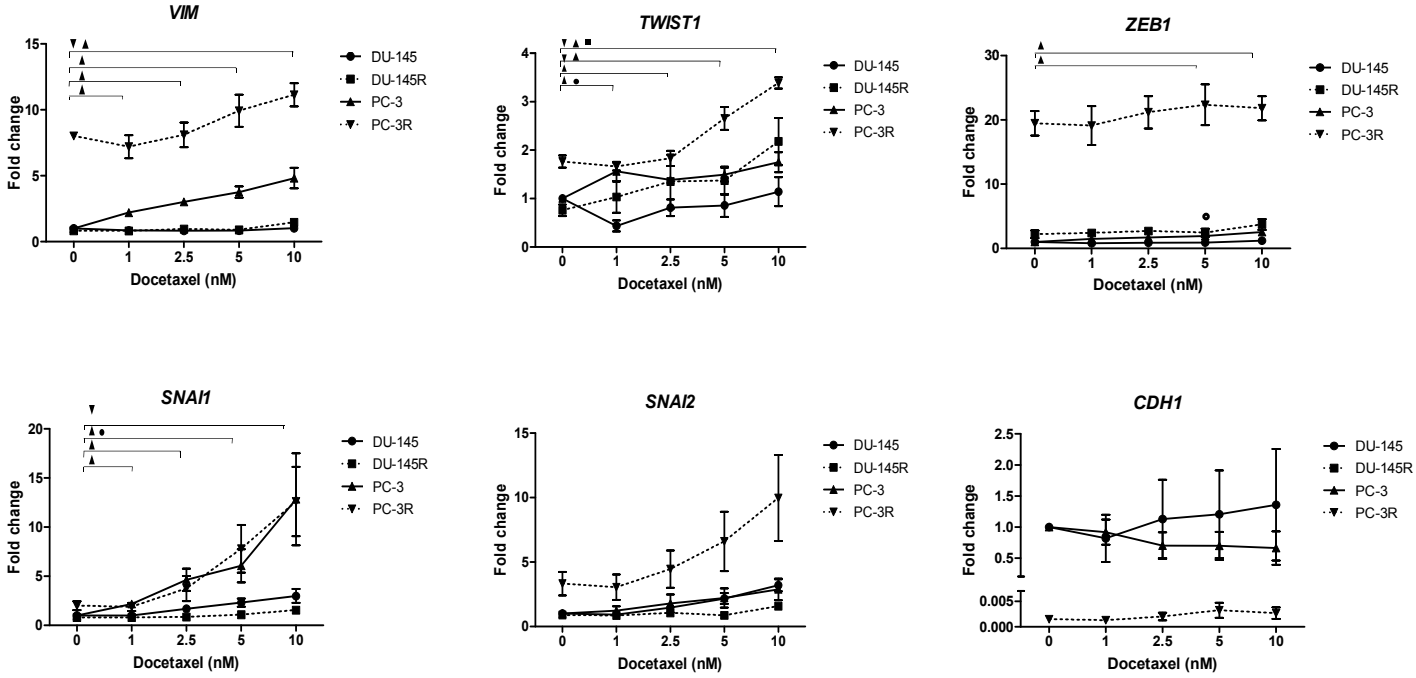

B

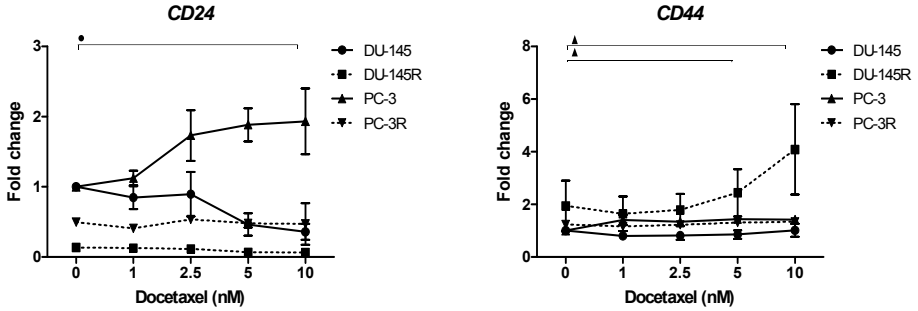

Author Manuscript Published OnlineFirst on March 21, 2014; DOI: 10.1158/1535-7163.MCT-13-0775
Author manuscripts have been peer reviewed and accepted for publication but have not yet been edited.

Figure 4